**Atmospheric
Chemistry
and Physics**

Technical Note: Use of a beam width probe in an Aerosol Mass Spectrometer to monitor particle collection efficiency in the field

D. Salcedo[1,2]**, T. B. Onasch**[3]**, M. R. Canagaratna**[3]**, K. Dzepina**[2,4]**, J. A. Huffman**[2,4]**, J. T. Jayne**[3]**, D. R. Worsnop**[3]**,
C. E. Kolb**[3]**, S. Weimer**[5,*]**, F. Drewnick**[6]**, J. D. Allan**[7]**, A. E. Delia**[8]**, and J. L. Jimenez**[2,4]

[1]Centro de Investigaciones Químicas, Universidad Autónoma del Estado de Morelos, Cuernavaca, Morelos, México
[2]Cooperative Institute for Research in the Environmental Sciences (CIRES), University of Colorado at Boulder, CO, USA
[3]Center for Aerosol and Cloud Chemistry, Aerodyne Research Inc., Billerica, MA, USA
[4]Department of Chemistry and Biochemistry, University of Colorado at Boulder, Boulder, CO, USA
[5]Atmospheric Sciences Research Center, University at Albany, Albany, NY, USA
[6]Particle Chemistry Department, Max Planck Institute for Chemistry, Mainz, Germany
[7]Department of Physics, University of Manchester Institute of Science and Technology, Manchester, UK
[8]Program in Atmospheric and Oceanic Sciences, University of Colorado at Boulder, Boulder, CO, USA
[*]now at: EMPA, Duebendorf, Switzerland and Paul Scherrer Institute, Villigen, Switzerland

Abstract. Two Aerodyne Aerosol Mass Spectrometers (Q-AMS) were deployed in Mexico City, during the Mexico City Metropolitan Area field study (MCMA-2003) from 29 March–4 May 2003 to investigate particle concentrations, sources, and processes. We report the use of a particle beam width probe (BWP) in the field to quantify potential losses of particles due to beam broadening inside the AMS caused by particle shape (nonsphericity) and particle size. Data from this probe show that no significant mass of particles was lost due to excessive beam broadening; i.e. the shape- and size-related collection efficiency (E_s) of the AMS during this campaign was approximately one. Comparison of the BWP data from MCMA-2003 with other campaigns shows that the same conclusion holds for several other urban, rural and remotes sites. This means that the aerodynamic lens in the AMS is capable of efficiently focusing ambient particles into a well defined beam and onto the AMS vaporizer for particles sampled in a wide variety of environments. All the species measured by the AMS during MCMA-2003 have similar attenuation profiles which suggests that the particles that dominate the mass concentration were internally mixed most of the time. Only for the smaller particles (especially below 300 nm), organic and inorganic species show different attenuation versus particle size which is likely due to partial external mixing of these components. Changes observed in the focusing of the particle beam in time can be attributed, in part, to changes in particle shape (i.e. due to relative humidity) and size of the particles sampled. However, the relationships between composition, atmospheric conditions, and particle shape and size appear to be very complex and are not yet completely understood.

1 Introduction

The Aerodyne Aerosol Mass Spectrometer (AMS) has been widely used to measure concentrations of non-refractory species in particles smaller than about 1 μm (NR-PM$_1$) with high time and size-resolution. However, in previous studies using the AMS (Allan et al., 2004; Drewnick et al., 2004b; Hogrefe et al., 2004; Zhang et al., 2005b) it has been observed that there is a systematic (but highly reproducible) underestimation of the mass concentration of aerosols measured with the AMS when compared to other quantitative aerosol measurements such as the Particle Into Liquid Sampler (PILS) or Scanning Mobility Particle Sizer (SMPS). In these studies, the underestimation in mass concentration observed with the AMS indicates AMS Collection Efficiencies (CE) ranging from 0.43 to 1.

Huffman et al. (2005) have recently defined the observed AMS collection efficiency as the product of three terms: $CE = E_L * E_s * E_b$. Previously, the latter two effects (and sometimes all three effects) had been included in one collection efficiency ($CE = E_s * E_b$ or $CE = E_L * E_s * E_b$) (Alfarra et al., 2004; Drewnick et al., 2004a; Zhang et al., 2004). The E_L term accounts for the fraction of particles in PM$_1$ that are not transmitted into the AMS due to limited transmission of

Correspondence to: J. L. Jimenez
(jose.jimenez@colorado.edu)

the inlet and lens of the AMS (Jayne et al., 2000; Zhang et al., 2004). E_s and E_b account for possible effects that cause non-detection of the PM_1 particles that are introduced into the instrument and exit the aerodynamic lens. The bounce-related collection efficiency (E_b) could be smaller than one if some of the dry less-volatile particles (such as those with a high proportion of $(NH_4)_2SO_4$) bounce after impacting the AMS vaporizer, instead of evaporating. The shape- and size-related collection efficiency (E_s) could be less than one for nonspherical particles because the efficiency with which they are focused by the lens is reduced due to lateral forces acting upon the particles during the acceleration in the lens (Jayne et al., 2000; Huffman et al., 2005). This could, in principle, cause some irregular particles to "miss" the AMS vaporizer.

While E_L is less than 1 at the small and large particle size ends of the aerodynamic lens transmission range due to spherical particle losses in the inlet and aerodynamic lens, E_S accounts for additional particle loss due to the potential inability of the aerodynamic lens to focus irregular particles onto the AMS vaporizer for detection. The latter effect may be important for particles less than 100 nm in diameter and is especially significant for sampling nanoparticles (Wang et al., 2005) because spherical particles at these sizes are less well focused by the lens, and any additional effect that degrades focusing (such as non-sphericity) is more likely to cause particle losses than for larger sizes which are very well focused.

The use of a particle beam width probe (BWP) to determine E_s in the laboratory (Jayne et al., 2000; Huffman et al., 2005) and in the field (Allan et al., 2006a; Weimer et al., 2006) has been described previously. However, this is the first report that analyzes in detail data from a BWP deployed in the field and compares the results obtained in several field studies.

The Mexico City Metropolitan Area field experiment (MCMA-2003) was an intensive 5-week campaign that took place in the spring of 2003 (31 March–4 May). It was conducted with the goal of investigating the atmospheric chemistry of the MCMA, with particular focus on emissions quantification, gas-phase photochemistry, and secondary particulate matter formation. During the MCMA campaign, we deployed two Aerodyne Quadrupole Aerosol Mass Spectrometers (Q-AMS); one at the CENICA supersite, located in the southeast area of Mexico City (Salcedo et al., 2006), and one on the Aerodyne Mobile Laboratory (Kolb et al., 2004). Both AMSs used a BWP to investigate the particle beam dispersion and to estimate the shape- and size-related collection efficiency of the Q-AMSs. In this paper, we briefly describe the BWP and analyze the particle beam width measurements as a function of relative humidity and particle size at the CENICA supersite and at La Merced, a site downtown Mexico City in an area of heavy vehicle traffic.

Results from beam width probe deployments at other sites in a wide variety of environments are briefly presented here and compared to the MCMA results:

1. New York City (NY): Q-AMS measurements were carried out during the Particulate Matter Technology Assessment and Characterization Study – New York (PMTACS-NY) 2004 winter campaign. The site was located in the campus of Queens College, within 1 km of two major traffic highways in the New York City metropolitan area (Weimer et al., 2006).

2. Duke Forest: the measurements were part of the Chemical Emission, Loss, Transformation and Interactions within Canopies (CELTIC) study, which took place during July 2003. The site was based at the Forest-Atmosphere Carbon Transfer and Storage (FACTS-I) facility located in the Blackwood Division of Duke Forest, near Durham, North Carolina. The forest is composed primarily of trees that emit both isoprene and terpenes, leading to likely formation of biogenic secondary organic aerosol. The site is also impacted by regional pollution transport (Delia, 2004).

3. Pinnacle Park: Pinnacle State Park in Addison, NY, is a rural site surrounded by a 9-hole golf course, a picnic area, undeveloped state forest lands, abandoned pastures, a 20 hectare pond, and a handful of homes. Measurements were part of the PMTACS-NY program in August 2004 (Schwab et al., 2006).

4. Chebogue Point: as part of the International Consortium for Atmospheric Research on Transport and Transformation (ICARTT) intensive field study during the summer of 2004, a fixed field site was operated at Chebogue Point. This was a remote site located on the coast of southern Nova Scotia which was designed to study the emissions from mainland North America within the boundary layer a period of hours to days after emission (Allan et al., 2006b[1]).

The particle beam width and the shape- and size-related collection efficiency (E_s) was calculated and compared at all the above sites to test the efficiency of the aerodynamic lens to focus the particles sampled in different environments.

2 Experimental

The Q-AMS has been described in detail previously (Jayne et al., 2000; Jimenez et al., 2003) and the details of its op-

---

[1]Allan, J. D., Coe, H., Cubison, M. J., Jimenez, J. L., Huffman, J. A., DeCarlo, P. F., Northway, M., Canagaratna, M. R., Onasch, T., Cross, E. S., Coulson, G., Zhang, Q., Goldstein, A. H., Williams, B. J., Millet, D. B., Ogren, J., Andrews, E., Sheridan, P., Jefferson, A., Roberts, J. M., Kreisberg, N. M., Hering, S. V., Russell, L., Gilardoni, S., Quinn, P., and Worsnop, D. R.: Overview of In Situ Measurements of Particle Composition at Chebogue Point, Nova Scotia, During Summer 2004 and Insights into Organic Chemical Processes, J. Geophys. Res., submitted, 2006b.
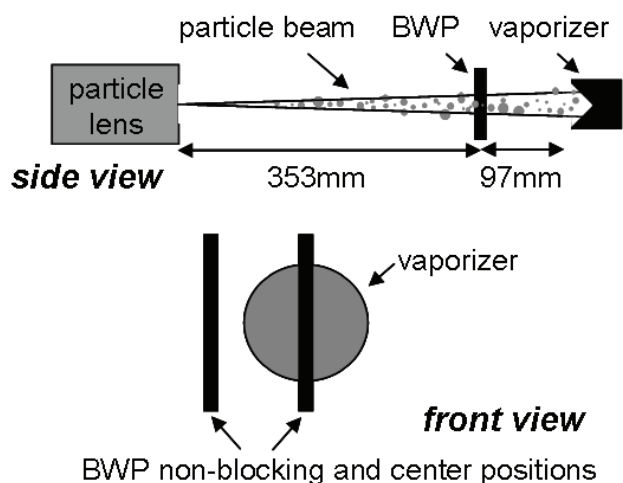
Fig. 1. Schematic diagram of the AMS vaporizer and Beam Width Probe (BWP). The dimensions in the figure correspond to a long chamber (Huffman et al., 2005).

Fig. 2. Average signal attenuation for the airbeam and the main AMS species measured at CENICA as a function of distance of the BWP from the center of the vaporizer. Nitrate, sulfate, and organics curves are not visible because they are behind the ammonium curve. The relative sizes of the vaporizer and the BWP (projected onto the plane of the vaporizer) are shown at the bottom of the figure.

eration and main results from the CENICA supersite are described elsewhere (Salcedo et al., 2006). The BWP was used to allow the estimation of the potentially reduced particle collection efficiency due to particle size and shape, as well as to study the degree of nonsphericity of the ambient aerosol. The design of the probe and the techniques for analysis and interpretation of its data have been extensively discussed elsewhere (Jayne et al., 2000; Huffman et al., 2005).

Figure 1 schematically shows the probe used at CENICA, which consisted of a 0.41 mm diameter wire which casts a "shadow" 0.52 mm wide at the surface of the vaporizer. The wire was moved intermittently to several fixed positions blocking different parts of the particle beam from reaching the AMS vaporizer, in order to determine the attenuation of the signal versus wire position. The BWP was alternated between the "out" position (not blocking any part of the vaporizer) and one of the seven partially blocking positions in front of the 3.81 mm diameter vaporizer. One of the seven blocking positions covered the center of the vaporizer and the other six were symmetrically located on each side of the beam center. When the BWP was on the center position, its shadow covered 21.8% of the total area of the vaporizer. The probe was moved every two minutes, with a total cycling time (rotating through the entire round of positions) of 28 min. Note that due to imperfections in the construction of the aerodynamic lens, different particle sizes can be focused along slightly different axis (Huffman et al., 2005), with this effect being more pronounced for the smaller particles transmitted by the lens. Since the alignment of the BWP and aerodynamic lens is always performed with particles in the accumulation mode size range, this may lead to a systematic bias with lower particle beam attenuation for the smaller particles.
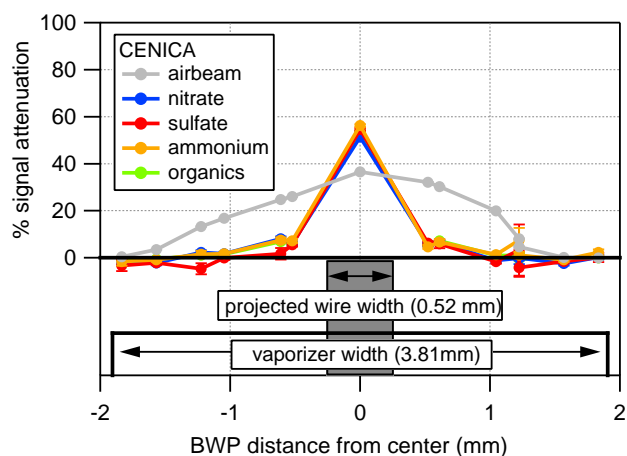
The Q-AMS has been deployed using a number of different configurations, with two different chamber lengths ("long" and "short") (Huffman et al., 2005), as well as several designs of the aerodynamic lens (Zhang et al., 2004). All the AMS instruments mentioned in this paper used a long chamber (see Fig. 1) and a "standard" aerodynamic lens. Although the operation of the BWP was similar in all the instruments, the diameter of the wire used was different. The wire used at NY and Pinnacle Park was 1.0 mm in diameter, while the wire used at La Merced, Duke Forest and Chebogue Point had a diameter of 0.5 mm.

3 Results and discussion

The time series of the signal attenuation at CENICA was calculated for each AMS species by comparing the particle signal when the wire was blocking the beam to the nonblocking position signals in the 2 minutes preceding and following the attenuated measurement. The average signal attenuation for each species measured as a function of BWP position across the particle beam is shown in Fig. 2. Non-refractory chloride is not included because its concentration was generally very low most of the time and its attenuated signal profile is very noisy. The attenuation at each position is similar for all species, and it is large only when the BWP is at the center position. This means that the particle beam is well-focused on the vaporizer, covering only a small area in the center of it. The area under the curve in Fig. 2 does not add up to 100%, as is expected if all the wire positions are situated next to each other, with no overlapping or gapping. The reason is that, due to an error in the wire mechanism setup, there were
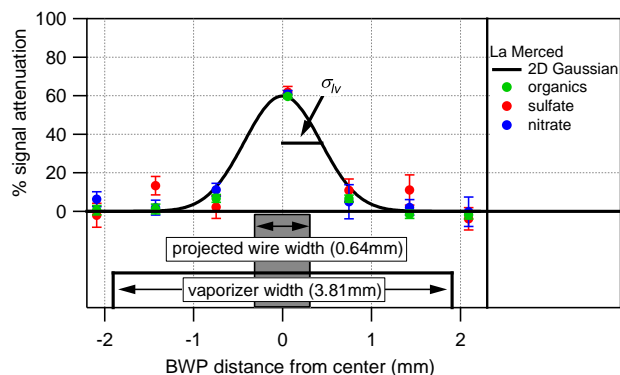
Fig. 3. Average signal attenuation for the main AMS species measured at La Merced as a function of distance of the BWP from the center of the vaporizer. Line: signal attenuation caused by a 0.5 mm wire, calculated using the 2-D Circular Gaussian model described by Huffman et al. (2005).

Fig. 4. Box-whisker plots of the beam width for several campaigns using Q-AMSs equipped with a BWP. Dots represent the average beam width (σ_{lv}); horizontal lines represent the median; bottom and top of the boxes represent the 25 and 75 percentiles, respectively; and the bottom and the top whiskers represent the 5 and 95 percentiles, respectively. On the right side, the shape- and size-related collection efficiency (E_s) as a function of beam width is shown.

small gaps between the middle wire positions that caused the wire not to cover 100% of the vaporizer area. The fact that the profiles in Fig. 2 of all species are similar suggests that the ambient particles that accounted for most of the submicron mass were typically internally mixed during MCMA-2003. Similar conclusions were obtained from the analysis of the speciated size distributions (Salcedo et al., 2006) and from electron microscopy studies of individual particles collected at the CENICA site (Johnson et al., 2005).

The airbeam signal (grey trace in Fig. 2) is attenuated at all positions except the outermost one, which indicates that the airbeam is not as well-focused as the particle beam. The attenuation of the airbeam is not symmetrical around the center of the AMS vaporizer. This asymmetry in the airbeam might be caused by slight imperfections in the apertures and skimmers that the airbeam traverses inside the AMS. These imperfections do not appear to significantly affect the particle beam focusing. Another possible cause of the slight asymmetry of the broad airbeam distribution is a potential asymmetry of the electron density in the ionizer, caused by the position of the filament. If that is indeed the case, the particle beams are probably too narrow and the resolution of the spatial measurements are too low to observe a similar asymmetry in the particle signal.

Huffman et al. (2005) have used a 2-D Circular Gaussian model to describe the particle density distribution (the beam shape) after the aerodynamic lens. Using this model, it is possible to determine the beam width at the vaporizer from the particle signal attenuation observed due to the BWP. Figure 3 shows the average signal attenuation for speciated mass loading measured at La Merced, compared with the expected attenuation for the 0.5 mm wire used, calculated using the 2-D Gaussian model. The beam width was fitted so that expected attenuation showed the best correlation with the field data. The plot for ammonium is not included because the
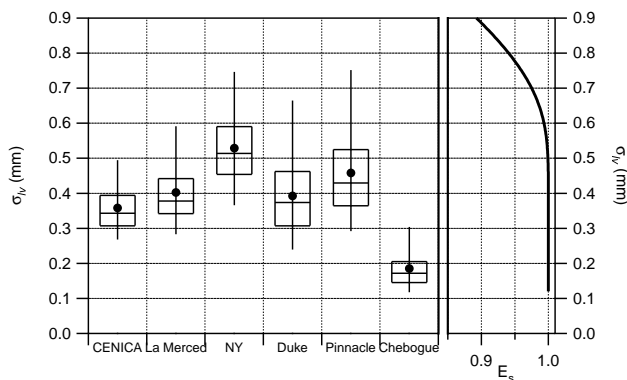
attenuation profile is noisier than for the other species due to higher noise at the mass peaks used by the AMS to quantify this species (mainly caused by interference from O^+ ions from O_2 and water with the NH_2^+ ions). However, the attenuation profile for ammonium is very similar to the profiles for nitrate and sulfate. The agreement between the observed and the expected attenuation due to the BWP indicates that the 2-D Gaussian model is consistent with the particle beam shapes observed for ambient particles.

Applying the 2-D Circular Gaussian model of Huffman et al. (2005) to the attenuation profile of the total AMS mass concentrations, we calculated the time dependent particle beam width at the vaporizer plane (σ_{lv}) for each of the campaigns listed above. σ_{lv} is the standard deviation for the 2-D Circular Gaussian function, centered at the axis defined by the lens and the center of the vaporizer, that describes the particle density distribution in the beam at the plane of the vaporizer of a long chamber AMS. Figure 3 shows the average σ_{lv} for the La Merced study. The resulting time dependent particle beam width was then averaged over all the sampling time in each study. The mean values, along with the median, and the 5, 25, 75, and 95 percentiles, are shown in Fig. 4. This figure also shows the relation between particle beam width and the shape- and size-related collection efficiency (E_s), (Fig. 4 in Huffman et al., 2005). The particle beam width values measured during MCMA-2003 correspond to a collection efficiency for the AMS vaporizer that is larger than 99% ($E_s \sim 1$). Thus, no significant particle mass went undetected because of excessive beam divergence. Although the other sites represent very different environments (one urban, two rural and one remote) with correspondingly different particle chemical compositions and size distributions, the AMS particle beam in nearly all cases was sufficiently well focused for complete collection at the vaporizer ($E_s \sim 1$).
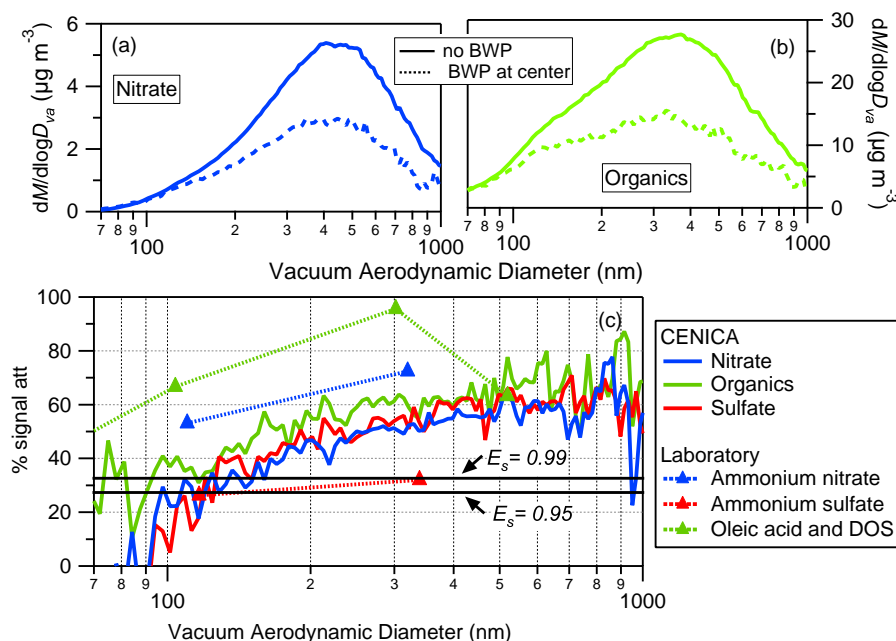
Fig. 5. Panels **(a)** and **(b)**: Campaign-average size distributions obtained by the AMS with the BWP in the non-blocking and particle beam center-blocking positions, measured at CENICA during MCMA-2003. Panels **(c)**: signal attenuation caused by the BWP at the center position as a function of particle size. Also included is data from laboratory experiments with ammonium nitrate, ammonium sulfate, oleic acid (Huffman et al., 2005), and DOS (Liu et al., 1995) particles.

Only few periods were observed during the NY and Pinnacle studies when the sampled particle beam widths were greater than 0.77 mm, corresponding to a loss of ∼5% of the particles due to inadequate focusing. Thus, the standard aerodynamic lens used in the AMS is capable of efficiently focusing the particles that dominate the mass distribution into a narrow particle beam, with particle mass losses due to inadequate focusing close to zero for a broad variety of different aerosols most of the time, with E_S rarely smaller than 0.95. Interestingly, the Chebogue data shows a very narrow beam most of the time. This is probably due to the relatively high RH during the campaign, because the site was within 100 m of the ocean and frequently under foggy conditions.

Particle beam focusing in aerodynamic lenses is known to be a function not only of shape, but also of particle size (Zhang et al., 2004; Huffman et al., 2005). In order to explore the focusing of the ambient particle beam as a function of particle size, panels (a) and (b) in Fig. 5 show the size distribution for particulate nitrate and organics at the CENICA site, compared with the size distribution measured when the BWP was blocking the center of the particle beam. Panel (c) in Fig. 5 shows the signal attenuation when the BWP was on the center position as a function of particle size for nitrate, organics and sulfate. The plot for ammonium is not included because of the reasons explained above. However, the attenuation profile for ammonium is very similar to the profiles for nitrate and sulfate. For the non-center wire positions, the measured attenuation was near zero and therefore no size-dependent attenuation was observed.

Panel (c) in Fig. 5 also shows the attenuation expected for monodisperse pure-component particles calculated from laboratory measurements (Liu et al., 1995; Huffman et al., 2005). The attenuation for oleic acid particles, which are spherical, represent the maximum attenuation expected for a given particle diameter. Ammonium nitrate and sulfate particles show less attenuation than oleic acid because they are crystalline solids (nonspherical), the effect being more pronounced for ammonium sulfate. Ambient particles generally show much less attenuation than spherical oleic acid, indicating that ambient particles are not spherical, and in between those observed in the laboratory for pure ammonium nitrate and ammonium sulfate, indicating that ambient non-sphericity falls in between that of those two types of pure particles. Figure 5 also reveals a size dependence of the BWP signal attenuation that is qualitatively similar for particles with a vacuum aerodynamic diameter (d_{va}) (DeCarlo et al., 2004) below 350 nm for all species in the laboratory and the field. Smaller ambient particles are not as well focused as spherical particles of the same size. This leads to a somewhat reduced E_s at small particle sizes ($d_{va} < \sim 120$ nm), which is of minor importance in terms of the total particle mass since a very small fraction of the mass is typically found at those small sizes.
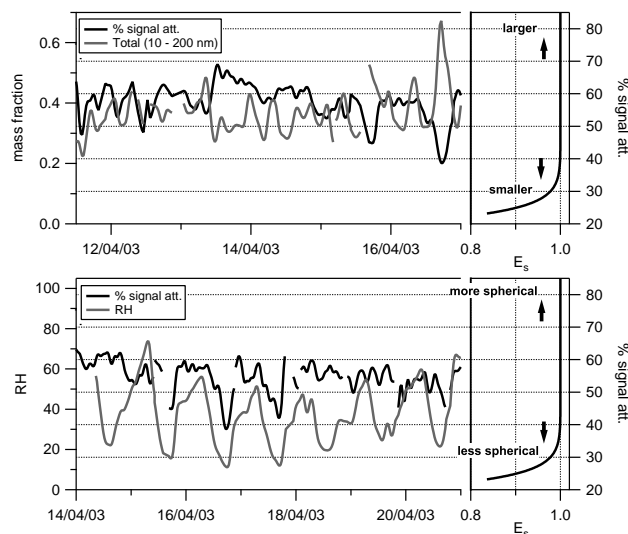
Fig. 6. Time series of the signal attenuation caused by the BWP at the center position, ambient RH and mass fraction of particles with $d_{va}<200$ nm, measured at CENICA during MCMA-2003. On the right side of both panels, E_s is shown as a function of signal attenuation, calculated using Huffman et al. (2005) model for the dimensions of the instrument and BWP used during this campaign (long chamber and a wire of 0.41 mm).

Zhang et al. (2004) estimated that spherical particles would suffer from incomplete collection below ~60 nm. Figure 5 suggests that the effect becomes important below ~120 nm due to the additional effects of nonsphericity. This is consistent with the observation by Salcedo et al. (2006) that the ultrafine particle mode is dominated by non-spherical combustion particles in Mexico City. Because the combustion-related organics are likely internally mixed with soot, these particles are often nonspherical and should form a wider beam, showing a lower attenuation. The attenuation of smaller particles is likely to be further reduced by the slight dependence of the particle focusing center on particle size, as discussed above. Thus, the particle beam widths and E_s deduced from these data should be considered upper and lower limits, respectively. Particles in the accumulation mode (300–800 nm) show much larger attenuation, indicating that they are better focused than the smaller particles. The similar attenuation of all species in the accumulation mode is again suggestive of internal mixing for this mode. However, for the smaller size range (<300 nm), the attenuation is different for the organics, sulfate and nitrate, which suggests that the organic and inorganic species in the smaller particles are at least partially externally mixed, again consistent with previous observations (Salcedo et al., 2006).

Figure 6 presents time series of the attenuation of the total signal at the CENICA site, caused by the BWP at the position that blocks the center of the particle beam. The data have been smoothed over time 5 points (~2 h) to reduce high-

Table 1. Correlation coefficients (r^2) calculated for the attenuation caused by the BWP at the center position vs. different parameters at the CENICA site during MCMA-2003. The data have been smoothed by 5 points (~2 h) before calculating r^2 to reduce high-frequency noise.

Parameter	Linear Correlation Coefficient (r^2)
RH	0.064
OOA fraction	0.033
HOA fraction	0.032
Mass fraction of particles with $d_{va}<200$ nm	0.026
Mass fraction of particles with $d_{va}>200$ nm	0.026
Sulfate fraction	0.022
BC fraction	0.009

frequency noise. The attenuation of the signal fluctuates in time, indicating changes in the particle beam focusing which might be attributed to changes in particle size distribution and the degree of nonsphericity. Only few days of the campaign are shown because the purpose of the figure is only to illustrate the range of variation of this measurement. The figure also illustrates the relation between the attenuation caused by a 0.41 mm wire and E_s from the model of Huffman et al. (2005).

In order to explore the relationship between particle shape and size and the BWP signal attenuation (i.e. with particle beam width), the relative humidity (RH) and the mass fraction of particles with $d_{va}<200$ nm are also shown in Fig. 6. RH is expected to correlate with particle shape because hygroscopic particles are likely liquid at higher RH leading to more spherical shapes (Allan et al., 2006a). Figure 6 shows that some of the variability in the signal attenuation appears to correlate with RH and some with the mass fraction of the smaller particles. However, these correlations do not always hold. Other parameters that may be correlated with particle sphericity or nonsphericity include mass fractions of oxygenated organic aerosol (OOA, which might be an indication of particle aging (Zhang et al., 2005a; Zhang et al., 2005c)), black carbon, sulfate, and hydrocarbon-like organic compounds (HOA, mostly primary combustion aerosol (Zhang et al., 2005c)). Table 1 shows correlation coefficients calculated for BWP attenuation vs. these parameters. None of these parameters explains more than 6.4% of the variance in the BWP signal attenuation. Similarly as for RH and smaller particle mass fraction, the correlation or anti-correlation between those parameters and signal attenuation is not always clear from their time series. These results indicate that multiple parameters may affect the measured signal attenuation (and thus particle beam width) in a complex way. In order to better understand this issue, detailed laboratory work with particles of known sizes, composition and shapes (e.g. combined with off-line electron microscopy measurements) as

well as under known RH conditions, and in-depth analysis of field data using multiple regression models need to be performed.

4 Conclusions

We report the use of a particle beam width probe inside two Q-AMSs in Mexico City during the MCMA-2003 field campaign to probe the surrogate shape of the particles, and to quantify potential losses of particles due to beam broadening. Results from these measurements show that the 2-D Circular Gaussian model of Huffman et al. (2005) is well suited to describe the particle distribution within the particle beam during ambient measurements. Particle losses due to dispersion of the beam were caused by shape and size of the particles and were very small ($E_s \sim 1$) in Mexico City during MCMA-2003. This is typically also true for other campaigns in various urban, rural and remote sites.

Attenuation of measured aerosol mass loading signals due to the BWP was similar for all the chemical species measured by the AMS, which is indicative of particles being internally mixed most of the time. Particles smaller than 300 nm exhibited somewhat different attenuations for the organic and inorganic components likely indicating partial external mixing of these smaller particle components. Observed attenuation of the ambient particles was found to be significantly lower than one would expect for spherical particles, and was generally between those determined for pure ammonium nitrate and ammonium sulfate particles in the laboratory. This also suggests internal mixture of the various aerosol components, resulting in moderately nonspherical particle shapes that produce intermediate particle beam broadening. Temporal variations in the BWP attenuation indicate changes in the particle beam focusing likely attributable to changes in the particle shape and size. However, the relationships among the particle shape, size and particle beam focusing are complex and more laboratory and field work is needed in order to better understand this issue.

References

Alfarra, M. R., Coe, H., Allan, J. D., Bower, K. N., Boudries, H., Canagaratna, M. R., Jimenez, J. L., Jayne, J. T., Garforth, A., Li, S. M., and Worsnop, D. R.: Characterization of Urban and Regional Organic Aerosols In the Lower Fraser Valley Using Two Aerodyne Aerosol Mass Spectrometers, Atmos. Environ., 38, 5745–5758, 2004.

Allan, J. D., Alfarra, M. R., Bower, K. N., Coe, H., Jayne, J. T., Worsnop, D. R., Aalto, P. P., Kulmala, M., Hyötyläinen, T., Cavalli, F., and Laaksonen, A.: Size and composition measurements of background aerosol and new particle growth in a Finnish forest during QUEST 2 using an Aerodyne Aerosol Mass Spectrometer, Atmos. Chem. Phys., 6, 315–327, 2006a.

Allan, J. D., Bower, K. N., Coe, H., Boudries, H., Jayne, J. T., Canagaratna, M. R., Millet, D. B., Goldstein, A. H., Quinn, P. K., Weber, R. J., and Worsnop, D. R.: Submicron aerosol composition at Trinidad Head, CA during ITCT 2K2, its relationship with gas phase volatile organic carbon and assessment of instrument performance, J. Geophys. Res., 109, D23S24, doi:10.1029/2003JD004208, 2004.

DeCarlo, P. F., Slowik, J. G., Worsnop, D. R., Davidovits, P., and Jimenez, J. L.: Particle Morphology and Density Characterization by Combined Mobility and Aerodynamic Diameter Measurements. Part 1: Theory, Aerosol Sci. Technol., 38, 1185–1205, doi: 10.1080/027868290903907, 2004.

Delia, A. E.: Real-Time Measurements of Non-Refractory Particle Composition and Interactions at Forested Sites, Ph.D. thesis, University of Colorado, Boulder, CO, 2004.

Drewnick, F., Jayne, J. T., Canagaratna, M. R., Worsnop, D. R., and Demerjian, K. L.: Measurement of Ambient Aerosol Composition During the PMTACS-NY 2001 Using an Aerosol Mass Spectrometer. Part II: Chemically Speciated Mass Distributions, Aerosol Sci. Technol., 38, 104–117, 2004a.

Drewnick, F., Schwab, J. J., Jayne, J. T., Canagaratna, M. R., Worsnop, D. R., and Demerjian, K. L.: Measurement of Ambient Aerosol Composition During the PMTACS-NY 2001 Using an Aerosol Mass Spectrometer. Part I: Mass concentrations, Aerosol Sci. Technol., 38, 92–103, doi:10.1080/02786820390229507, 2004b.

Hogrefe, O., Schwab, J. J., Drewnick, F., Lala, G. G., Peters, S., Demerjian, K. L., Rhoads, K., Felton, H. D., Rattigan, O. V., Husain, L., and Dutkiewicz, V. A.: Semicontinuous $PM_{2.5}$ Sulfate and Nitrate Measurements at an Urban and a Rural Location in New York: PMTACS-NY Summer 2001 and 2002 Campaigns, J. Air. Waste Manage., 54, 1040–1060, 2004.

Huffman, J. A., Jayne, J. T., Drewnick, F., Aiken, A. C., Onasch, T., Worsnop, D. R., and Jimenez, J. L.: Design, Modeling, Optimization, and Experimental Tests of a Particle Beam Width Probe for the Aerodyne Aerosol Mass Spectrometer, Aerosol Sci. Technol., 39, 1143–1163, 2005.

Jayne, J. T., Leard, D. C., Zhang, X., Davidovits, P., Smith, K. A., Kolb, C. E., and Worsnop, D. R.: Development of an Aerosol Mass Spectrometer for Size and Composition Analysis of Submicron Particles, Aerosol Sci. Technol., 33, 49–70, 2000.

Jimenez, J. L., Jayne, J. T., Shi, Q., Kolb, C. E., Worsnop, D. R., Yourshaw, I., Seinfeld, J. H., Flagan, R. C., Zhang, X., Smith, K. A., Morris, J., and Davidovits, P.: Ambient aerosol sampling using the Aerodyne Aerosol Mass Spectrometer, J. Geophys. Res., 108, 8425, doi:10.1029/2001JD001213, 2003.

Johnson, K. S., Zuberi, B., Molina, L. T., Molina, M. J., Iedema, M. J., Cowin, J. P., Gaspar, D. J., Wang, C., and Laskin, A.: Processing of soot in an urban environment: case study from the Mexico City Metropolitan Area, Atmos. Chem. Phys., 5, 3033–3043, 2005, http://www.atmos-chem-phys.net/5/3033/2005/.

Kolb, C. E., Herndon, S. C., McManus, J. B., Shorter, J. H., Zahniser, M. S., Nelson, D. D., Jayne, J. T., Canagaratna, M. R., and Worsnop, D. R.: Mobile Laboratory with Rapid Response Instruments for Real-Time Measurements of Urban and Regional Trace Gas and Particulate Distributions and Emission Source Characteristics, Environ. Sci. Technol., 38, 5694–5703, 2004.

Liu, P., Ziemann, P. J., Kittelson, D. B., and McMurry, P. H.: Generating particle beams of controlled dimensions and divergence. 2. Experimental evaluation of particle motion in aerodynamic lenses and nozzle expansions, Aerosol Sci. Technol., 22, 314–324, 1995.

Salcedo, D., Onasch, T. B., Dzepina, K., Canagaratna, M. R., Zhang, Q., Huffman, J. A., DeCarlo, P. F., Jayne, J. T., Mortimer, P., Worsnop, D. R., Kolb, C. E., Johnson, K. S., Zuberi, B., Marr, L. C., Volkamer, R., Molina, L. T., Molina, M. J., Cardenas, B., Bernabé, R. M., Márquez, C., Gaffney, J. S., Marley, N. A., Laskin, A., Shutthanandan, V., Xie, Y., Brune, W., Lesher, R., Shirley, T., and Jimenez, J. L.: Characterization of ambient aerosols in Mexico City during the MCMA-2003 campaign with Aerosol Mass Spectrometry: results from the CENICA Supersite, Atmos. Chem. Phys., 6, 925–946, 2006, http://www.atmos-chem-phys.net/6/925/2006/.

Schwab, J. J., Felton, H. D., Rattigan, O. V., and Demerian, K. L.: New York State Urban and Rural Measurements of Continuous PM2.5 Mass by FDMS, TEOM, and BAM., J. Air. Waste Manage., 56, 372–383, 2006.

Wang, X., Kruis, F. E., and McMurry, P. H.: Aerodynamic Focusing of Nanoparticles: I. Guidelines for Designing Aerodynamic Lenses for Nanoparticles, Aerosol Sci. Technol., 39, 611–623, 2005.

Weimer, S., Drewnick, F., Hogrefe, O., Schwab, J. J., Rhoads, K., Orsini, D., Canagaratna, M. R., Worsnop, D. R., and Demerjian, K. L.: Size-Selective Non-Refractory Ambient Aerosol Measurements during the PMTACS-NY 2004 Winter Intensive in New York City, J. Geophys. Res., 111, D18305, doi:10.1029/2006JD007215, 2006.

Zhang, Q., Alfarra, M. R., Worsnop, D. R., Allan, J. D., Coe, H., Canagaratna, M. R., and Jimenez, J. L.: Deconvolution and Quantification of Hydrocarbon-like and Oxygenated Organic Aerosols Based on Aerosol Mass Spectrometry, Environ. Sci. Technol., 39, 4938–4952, doi:10.1021/es048568l, 2005a.

Zhang, Q., Canagaratna, M. R., Jayne, J. T., Worsnop, D. R., and Jimenez, J. L.: Time and Size-Resolved Chemical Composition of Submicron Particles in Pittsburgh. Implications for Aerosol Sources and Processes, J. Geophys. Res., 110, D07S09, doi:10.1029/2004JD004649, 2005b.

Zhang, Q., Worsnop, D. R., Canagaratna, M. R., and Jimenez, J. L.: Hydrocarbon-like and Oxygenated Organic Aerosols in Pittsburgh: Insights into Sources and Processes of Organic Aerosols, Atmos. Chem. Phys., 5, 3289–3311, 2005c.

Zhang, X., Smith, K. A., Worsnop, D. R., Jimenez, J. L., Jayne, J. T., Kolb, C. E., Morris, J., and Davidovits, P.: Characterization of Particle Beam Collimation. Part II: Integrated Aerodynamic Lens-Nozzle System, Aerosol Sci. Technol., 38, 619–638, 2004.